The Titan N/N and C/C isotopic ratios in HCN from Cassini/CIRS

Sandrine Vinatier, Bruno Bézard, Conor A. Nixon

Accepted Manuscript

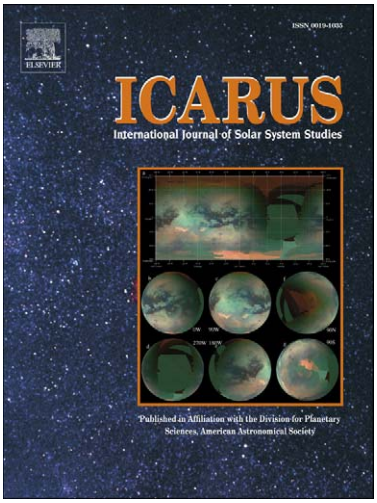

The Titan $^{14}N/^{15}N$ and $^{12}C/^{13}C$ isotopic ratios in HCN from Cassini/CIRS

Sandrine Vinatier, Bruno Bézard, Conor A. Nixon

PII: S0019-1035(07)00261-8
DOI: 10.1016/j.icarus.2007.06.001
Reference: YICAR 8308

To appear in: *Icarus*

Received date: 20 February 2007
Revised date: 30 May 2007
Accepted date: 3 June 2007

Please cite this article as: S. Vinatier, B. Bézard, C.A. Nixon, The Titan $^{14}N/^{15}N$ and $^{12}C/^{13}C$ isotopic ratios in HCN from Cassini/CIRS, *Icarus* (2007), doi: 10.1016/j.icarus.2007.06.001

The Titan $^{14}N/^{15}N$ and $^{12}C/^{13}C$ isotopic ratios in HCN from Cassini/CIRS

Sandrine Vinatier[1], Bruno Bézard[1], Conor A. Nixon[2]

[1] LESIA, Observatoire de Paris, 5 place Jules Janssen, F-92195 Meudon, France

[2] Department of Astronomy, University of Maryland, College Park, MD 20742, USA

Pages: 34

Table : 1

Figures: 8

Proposed Running Head: Titan's $^{14}N/^{15}N$ and $^{12}C/^{13}C$ isotopic ratios in HCN

Editorial correspondence to:

Sandrine Vinatier

LESIA - Observatoire de Meudon

5 place Jules Janssen

F-92195 Meudon, France

Phone: +33-1-45-07-77-30

Fax: +33-1-45-34-76-83

E-mail address: sandrine.vinatier@obspm.fr

ABSTRACT

We report the detection of $H^{13}CN$ and $HC^{15}N$ in mid-infrared spectra recorded by the Composite Infrared Spectrometer (CIRS) aboard Cassini, along with the determination of the $^{12}C/^{13}C$ and $^{14}N/^{15}N$ isotopic ratios. We analyzed two sets of limb spectra recorded near 13-15°S (Tb flyby) and 83°N (T4 flyby) at 0.5 cm^{-1} resolution. The spectral range 1210-1310 cm^{-1} was used to retrieve the temperature profile in the range 145-490 km at 13°S and 165-300 km at 83°N. These two temperature profiles were then incorporated in the atmospheric model to retrieve the abundance profile of $H^{12}C^{14}N$, $H^{13}CN$ and $HC^{15}N$ from their bands at 713, 706 and 711 cm^{-1} respectively. The HCN abundance profile was retrieved in the range 90-460 km at 15°S and 165-305 km at 83°N. There is no evidence for vertical variations of the isotopic ratios. Constraining the isotopic abundance profiles to be proportional to the HCN one, we find $^{12}C/^{13}C = 89^{+22}_{-18}$ at 15°S, and 68^{+16}_{-12} at 83°N, two values that are statistically consistent. A combination of these results yields a $^{12}C/^{13}C$ value equal to 75 ± 12. This global result, as well as the 15°S one, envelop the value in Titan's methane (82.3±1, Niemann et al., 2005) measured at 10°S and is slightly lower than the terrestrial inorganic standard value (89). The $^{14}N/^{15}N$ isotopic ratio is found equal to 56^{+16}_{-13} at 15°S and 56^{+10}_{-9} at 83°N. Combining the two values yields $^{14}N/^{15}N = 56$ ± 8, which corresponds to an enrichment in ^{15}N of about 4.9 compared with the terrestrial ratio. These results agree with the values obtained from previous ground-based millimeter observations (Hidayat et al., 1997; Marten et al. 2002). The $^{15}N/^{14}N$ ratio found in HCN is ∼3 times higher than in N_2 (Niemann et al., 2005), which implies a large fractionation process in the HCN photochemistry.

Key words: Titan; Abundances, atmosphere; Infrared observations

1 Introduction

The complex chemistry of Titan's atmosphere was first revealed by Voyager 1 in 1980. It is initiated by the ultraviolet and electron dissociation of its two major constituents, CH_4 and N_2, and leads to a suite of hydrocarbons and nitriles. The most abundant nitrile in Titan is HCN (hydrogen cyanide). A vertical profile of this molecule was first determined from Voyager 1 limb data at 70°N with a vertical resolution of about 200 km (Coustenis et al., 1991). HCN was also detected from Earth through millimeter observations, and the most recent studies of this molecule were done by Hidayat et al. (1997), Marten et al. (2002) and Gurwell (2004), who provided disk-averaged vertical mixing ratio profiles.

Millimeter observations allowed the authors to estimate the $^{12}C/^{13}C$ and $^{14}N/^{15}N$ isotopic ratio in HCN. The spread in the ground-based $^{12}C/^{13}C$ ratio deduced by Hidayat et al. and Gurwell (see Table 1) is large enough to encompass the terrestrial inorganic standard reference value (equal to 89, Fegley 1995). In situ measurements realized by the Huygens/GCMS and the Cassini/INMS instruments yield comparable $^{12}C/^{13}C$ isotopic ratios in CH_4 that are slightly lower than the terrestrial value (Niemann et al. 2005 and Waite et al. 2005, see Table 1). Consequently, the $^{13}C/^{12}C$ isotopic ratio in HCN does not seem to be strongly enriched compared to CH_4. As HCN is formed from the dissociation of N_2 and CH_4, the latter being the main reservoir of carbon in Titan's atmosphere, these results imply that carbon does not undergo significant fractionation in the HCN formation process. Moreover, both the relatively short lifetime of methane in Titan's atmosphere ($\sim$100 Myr, Yung et al. 1984; Wilson and Atreya, 2004) and the small enrichment of the $^{13}C/^{12}C$ ratio compared with the $^{15}N/^{14}N$ ratio in N_2 suggest a continuous or periodic replenishment of CH_4 on Titan at a rate higher than the escape rate.

Marten et al. (2002), using ground-based millimeter observations, showed that the $^{15}N/^{14}N$ ratio in HCN is enhanced by a factor lying in the range 3.9 - 4.5 compared to

the terrestrial value ($(^{14}N/^{15}N)_{\oplus}$ = 272, Fegley 1995). Gurwell (2004) also evaluated the $HC^{14}N/HC^{15}N$ ratio and concluded that ^{15}N was enriched by a factor of 2.9 - 3.8 times the Earth value (see Table 1). The nitrogen isotopic ratio was also determined from in situ data recorded by the GCMS. Niemann et al. (2005) retrieved a $^{14}N/^{15}N$ ratio in N_2 equal to 183 $\pm$ 5, lower than the terrestrial value by a factor $\sim$ 1.5. Waite et al. (2005), using Cassini/INMS in situ measurements at 1200 km, estimated this same isotopic ratio, and derived results in agreement with the GCMS one (see Table 1). Therefore, the $^{15}N/^{14}N$ ratio in N_2 (the main reservoir of nitrogen in Titan) is about 3 times lower than measured in HCN. This implies that a fractionation process exists in the HCN chemistry and favors the $HC^{15}N$ isotope. From the $^{15}N/^{14}N$ isotopic ratio derived in HCN (4.5 times the terrestrial value), Lunine et al. (1999) estimated that the primitive atmosphere of Titan was 20 to 100 times more massive than today. Using $^{15}N/^{14}N = 1.5\times(^{15}N/^{14}N)_{\oplus}$, Niemann et al. (2005) re-evaluated the mass of the primitive atmosphere to be between 2 and 10 times today's value while Waite et al. (2005) conclude that Titan's atmosphere was at least 50 % denser in the past. Most of this primitive atmosphere was thus lost by atmospheric escape over geological times (Lunine et al., 1999).

We report here the detection of $H^{13}CN$ and $HC^{15}N$ in the thermal infrared region from spectra recorded by the infrared spectrometer Cassini/CIRS, which allows for a new determination of the $^{14}N/^{15}N$ and $^{12}C/^{13}C$ ratios in HCN. We analyze spectra recorded at 13-15°S and 83°N and we investigate the vertical and latitudinal variations of these isotopic ratios. Section 2 presents the observational datasets. Principles of the HCN, $HC^{15}N$ and $H^{13}CN$ mixing ratio profile retrievals, as well as the results, are given in Section 3 and a discussion is presented in Section 4.

2 Observations

CIRS incorporates 3 focal planes, which cover all together the range 7 μm - 1 mm. Focal plane 1 (FP1), with a 3.9-mrad circular field of view (2.5 mrad at FWHM), records spectra in the far-infrared between 10 and 600 cm^{-1} (17-1000 μm). The mid-infrared region is covered by Focal Plane 3 (FP3) and Focal Plane 4 (FP4), which measure the spectral ranges 600-1100 cm^{-1} (9 to 17μm) and 1100-1500 cm^{-1} (7 to 9 μm) respectively. FP3 and FP4 consist of two parallel linear arrays each composed of ten detectors, with a field of view of 0.273 mrad per detector. This configuration is particularly suitable for limb observations, as the arrays are positioned along a Titan radius, so that each detector has a line of sight probing a particular level (at the tangent height) in Titan's atmosphere. Levels in the lower stratosphere, optically thick in a limb-viewing geometry, can be sounded by nadir observations, albeit with a lower vertical resolution. More details about CIRS are given in Kunde et al. (1996) and Flasar et al. (2004).

2.1 The 15°S selection (Tb flyby)

The first set of limb spectra that we used in this study was acquired during the Tb flyby, on 13 December 2004, with long integration limb observations performed at 0.5 cm^{-1} resolution by FP3 and FP4 over latitudes of 15°S and 13°S respectively. The mean vertical resolution of the observations, limited by the pixel angular size, is about 33 km. We averaged the individual spectra ($\sim$27) recorded by each detector. Eight selections of FP3 spectra were used at mean nominal altitudes of 212, 248, 284, 320, 355, 391, 427 and 463 km; for FP4, the altitudes of the averaged spectra were 205, 240, 276, 312, 348, 384, 420 and 456 km.

We also used selections of 80 nadir spectra recorded by FP3 and FP4 at mean latitudes of 12°S and 9°S respectively with a mean emission angle of 37°.

These selections are described in more detail in Vinatier et al. (2007).

2.2 The 83°N selection (T4 flyby)

The second set of limb spectra we analyzed here was acquired during the T4 flyby, on 1 April 2005, over a latitude of 83°N at a resolution of 0.5 cm^{-1}. In contrast to the Tb observations, the vertical resolution of the T4 observations was approximately 10 km. T4 limb spectra are distributed roughly homogeneously in height, so that we averaged spectra in adjacent 20-km bins, which yields an averaged value of 10 spectra per bin. The nominal altitudes of the FP3 and FP4 spectral averages are almost the same and equal to 159, 178, 201, 218, 239, 260, 281 and 298 km.

We did not use nadir observations in our analysis of T4 data for two reasons. The first one is that no nadir spectra were recorded at latitudes above 75°N, and that, at these very high latitudes, the meridional variation of temperature (and probably abundance) seems to be significant in a 5° range (Flasar et al. 2005). The second reason is connected to the high values of emission angles near the north pole (orbits of the spacecraft were still very close to Titan's orbiting plane), so that such observations do not effectively probe levels below those probed by the limb viewing geometry.

3 HCN, $H^{13}CN$ and $HC^{15}N$ mixing ratio retrievals

Emission band intensity depends on both temperature and molecular abundances. Therefore, the determination of the vertical abundance profile requires the knowledge of the temperature profile as a first step.

3.1 Temperature profile retrieval

The vertical temperature profile is determined by using the ν_4 methane (CH_4) emission band at 1305 cm^{-1} (7.7 μm) at several altitudes, and by assuming that the CH_4 abundance is constant in the whole stratosphere and equal to 1.41 %, as inferred from the GCMS data (Niemann et al., 2005). We use a constrained linear inversion algorithm combining both nadir and limb spectra as described in Vinatier et al. (2007). The principle of the temperature retrieval consists in the modification of an initial temperature profile by the algorithm to minimize the quadratic difference (χ^2) between measured and calculated spectra while not moving too far from the reference profile. The new calculated temperature profile is then used as a first guess of a new iteration process. After 3 iterations, the convergence is ensured, as the χ^2 no longer significantly decreases afterwards. The spectral interval used in the ν_4 CH_4 band is 1215-1309 cm^{-1}, which covers the Q- and P-branches. CH_4 spectroscopic parameters are extracted from the Geisa 2003 database (Jacquinet-Husson et al. 2005). Collision-induced opacity from N_2-N_2, N_2-CH_4, N_2-H_2 and CH_4-CH_4 are included in the model.

A vertical filtering of the solution is applied and characterized by a correlation length equal to 1 scale height at both latitudes. Parts of the temperature profiles that are not constrained by data blend smoothly in with the initial guess profile used in the retrieval algorithm. The radiative transfer model and the retrieval algorithm are described in more detail in Vinatier et al. (2007).

In the ν_4 CH_4 band, a continuum emission from the stratospheric haze is visible between the CH_4 multiplets, especially in limb spectra. We used the same haze model based on the DISR/Huygens results (Tomasko et al. 2005) as described in Vinatier et al. (2007), i.e. the haze optical depth is assumed to decrease slowly with height, varying as $p^{0.1}$, up to the 1-mbar level. Above this level, the haze opacity decreases with altitude with the pressure

scale height. We adjusted the integrated haze opacity (down to the surface) in order to fit the emission between the CH_4 multiplets in the low frequency wing of the P-branch.

We used the temperature profile deduced from HASI data (Fulchignoni et al. 2005) as an initial guess in the retrieval of our temperature profile at 13°S. At 83°N, our initial thermal profile was equal to the temperature profile retrieved at 80°N by Vinatier et al. (2007). Because no data were available at this latitude above the 0.01-mbar level (300 km), the stratopause in the retrieved thermal profile is not constrained.

[**Figure 1**]

The retrieved temperature profiles are plotted in Fig. 1. The 13°S profile (solid black line) displays information between 3 mbar (145 km) and 0.002 mbar (490 km), and at 83°N, it is constrained between 1 mbar (165 km) and 0.05 mbar (300 km). Error bars are given at pressures that correspond to the maxima of the inversion kernels at 1305 cm^{-1}. These error bars are the quadratic sum of an error due to noise and another one due to limb altitude uncertainties (see below for more details). Error bars due to noise are calculated from the correlation matrices in the inversion algorithm, based on the noise equivalent spectral radiance (NESR) of the spectra, which is estimated from deep space spectra. As the rms of the residuals of the fits are always systematically larger than the NESR, we scaled this error by the factor rms/NESR (see Vinatier et al. 2007 for more details). We did not take into account the uncertainty of the methane abundance ($1.41\pm0.07\times10^{-2}$, Niemann et al. 2005), because it has a very small effect, within the error arising from the other sources.

In our temperature retrieval, we applied a correction in height that results from both the pointing error of CIRS and assumptions in the temperature profile at deeper levels that are not constrained by CIRS data. We were able to determine this correction by fitting the P- and Q-branches of the ν_4 CH_4 band, as the shape of the Q-branch and also the relative intensity of the P-(or R-) and Q-branches are very sensitive to the viewing

altitude. The method used here is the same as in Vinatier et al. (2007). For the Tb profile (13°S), we found a correction of +30 ±7 km compared to nominal data. For T4 (83°N), the correction was +5 ±7 km. The altitudes indicated in the figures of this paper take account of this altitude shift. More details about this altitude correction and its effect are given in Vinatier et al. (2007).

Another important point concerns the retrieval of the temperature profile at 83°N. The Q-branch is optically thick on several averaged limb spectra and the deepest level probed is around 0.13 mbar (250 km), whereas the P-branch is optically thin down to the 1-mbar level (164 km). As a result, and particularly for the Q-branch, the region of maximum information is not located around the tangent point, but closer to the spacecraft along the ray path and therefore at higher altitude. Since Cassini orbits were nearly in Titan's orbital plane during the two flybys studied here, such limb observations acquired near 83°N probed lower latitudes (down to 69°N, as calculated from the geometry of the ray path). As a consequence, the temperature profile below 250 km is a "composite" profile that includes information from the Q-branch originating from latitudes less than 83°N, and information from the P-branch related to the latitudes at the tangent points (i.e. 83°N). This problem is much less pronounced for targeted latitudes close to the equator (which is the case for Tb) because the limb observation geometry is different: the probed latitude does not vary significantly (even for optically thick lines of sight), whereas the longitude does. Previous studies showed that temperature and abundance present small longitudinal variations (Flasar et al. 2005; Teanby et al. 2006, Coustenis et al. 2007) but large latitudinal variations, especially towards high latitudes.

3.2 Mixing ratio profile retrieval

The retrieved thermal profile is then used to model observed spectra in the range 700-730 cm^{-1}, which includes the emission bands of $H^{12}C^{14}N$ (713 cm^{-1}), $H^{13}CN$ (706 cm^{-1}), and $HC^{15}N$ (711 cm^{-1}). Mixing ratio profiles were derived from limb and nadir spectra by using the same inversion method as for temperature (described above), but by replacing the temperature by the logarithm of the mixing ratio of the absorbers studied (see also Vinatier et al., 2007 for more details concerning the method). Up to three vertical profiles can be retrieved at the same time by the algorithm. To reproduce satisfactorily the continuum between molecular emission bands, we always retrieve the haze vertical opacity profile simultaneously with the mixing ratio profiles of the molecules we consider. We treat the haze opacity as solely absorption with no scattering, and assume a gray variation in each spectral range considered for the retrievals.

Synthetic spectra and inversion kernels are computed from a line-by-line radiative transfer program. Collision-induced opacity from N_2-N_2, N_2-CH_4, N_2-H_2 and CH_4-CH_4 was included in the model. HCN spectroscopic parameters were extracted from HITRAN 2004 (Rothman et al. 2005), which includes the $H^{13}CN$ and $HC^{15}N$ isotopes. We assume that these two isotopes follows the same saturation law as HCN in the lower part of the stratosphere. In the spectral range studied here (700-730 cm^{-1}), C_2H_2 also displays many strong emission features from its ν_5 band (with its Q-branch at 729 cm^{-1}). Its spectroscopic parameters were extracted from the Geisa 2003 database (Jacquinet-Husson et al. 2005). Therefore, we first retrieved the mixing ratio profiles of C_2H_2 at both latitudes and incorporated them in the atmospheric models used to retrieve the mixing ratio profile of HCN and its two isotopes.

A vertical filtering of the solution is applied with a correlation length equal to 3 scale

heights at 15°S and 4 scale heights at 83°N for HCN and its 2 isotopes. This choice avoids the presence of strong oscillations on the retrieved vertical abundance profiles that appear with lower vertical filtering (e.g. of about 1 scale height). Arguments for this choice are detailed in Vinatier et al. (2007). The main point is that this large filtering does not significantly degrade the fits beyond the noise level.

3.3 Results

Figures 2 and 3 show some fits of the observed spectra at 15°S and 83°N in the spectral range 701-718 cm^{-1}. Comparisons of observed spectra with spectra calculated without the HCN isotope emission bands (solid gray line) and synthetic spectra including them (solid black lines) clearly validate the detection of $H^{13}CN$ and $HC^{15}N$ in the nadir and several limb spectra. Note that the altitudes are corrected by the same altitude shift as deduced from the ν_4 CH_4 band (see above).

[**Figures 2 and 3**]

3.3.1 The $H^{12}C^{14}N$ retrieved vertical profile

The inversion kernels of HCN are plotted in Figs. 4 and 5, at 15°S and 83°N respectively. The inversion kernels give the dependence of the emitted intensity upon the logarithm of the mixing ratio as a function of altitude and thus represent the information content of the spectra. In each figure, the HCN inversion kernels calculated at 712.25 cm^{-1} (dashed line) are plotted in both panels for comparison with the $H^{13}CN$ kernels at 706 cm^{-1} (left panel, solid gray line) and $HC^{15}N$ kernels at 711.25 cm^{-1} (right panel, solid gray line) calculated with isotope abundance profiles proportional to the HCN one (see Section 3.3.2).

[**Figures 4 and 5**]

At 15°S, we used both nadir and limb spectra to retrieve the abundance profile of HCN

and its isotopes. At 712.25 cm^{-1} (HCN Q-branch), the nadir spectrum probes levels (given by the full width of the kernels at half maximum) between 14 mbar (87 km) and 0.7 mbar (206 km) with a maximum at 3 mbar (37 km). To retrieve the HCN profile, we used 7 limb spectra that probe levels between 0.3 mbar (244 km) and 0.004 mbar (462 km).

At 83°N, HCN was inverted from 8 limb spectra probing levels between 0.95 mbar (165 km) and 0.05 mbar (305 km). Its emission is optically thin on all limb spectra. Note that the temperature profile at 83°N probes a large latitude range (between 69°N and 83°N) below the 250 km level (0.13 mbar), which may introduce some uncertainties on the abundance profile below this level.

Figure 6 gives the vertical profiles of HCN retrieved at 15°S and 83°N. Error bars for HCN are given at levels where its kernels are maximal. Note that the errors are correlated over ∼3 scale heights due to the filtering of the solution. These errors are the quadratic sum of an error due to noise, temperature uncertainties, and uncertainties in the altitude correction (see Section 3.1) equal to about ±7 km. Uncertainties due to noise are calculated in the same way as for the temperature profile, and we also multiplied this error by the factor rms/NESR. The error due to temperature uncertainties is estimated by retrieving extreme abundance profiles that use the minimum and maximum temperature profiles (defined by the temperature errors, see Fig. 1). The estimation of errors due to the altitude correction is performed by retrieving the abundance profile successively with the +7 km and -7 km shift while using the inverted temperature profile with the corresponding viewing altitudes.

[**Figure 6**]

3.3.2 Isotopic ratio vertical variations

We investigated the vertical variation of the $H^{13}CN$ and $HC^{15}N$ mixing ratio and found that vertical profiles proportional to the HCN one yield good fits of the data. The results of this analysis concerning $^{15}N/^{14}N$ are given in Fig. 7, which displays the comparison between two $^{15}N/^{14}N$ isotopic ratio vertical distributions calculated at 15°S. The first one, in solid black line, is deduced from HCN and $HC^{15}N$ vertical mixing ratio profiles retrieved with a correlation length equal to 3 scale heights (L=3). The second one, in dotted-dashed line, is deduced from the same retrieved HCN vertical abundance profile but with a $HC^{15}N$ mixing ratio profile proportional to the HCN one (i.e. L=∞), which yields to a constant $^{15}N/^{14}N$ ratio with height. Taken at face value, the isotopic ratio profile retrieved with L=3 would suggest an increase of the $^{15}N/^{14}N$ ratio by a factor of 1.7 between 200 and 300 km. However, the error bars are rather large and the two retrieved isotopic ratio profiles with L=3 and L=∞ yield similar fits of the data and almost the same reduced χ^2 (χ^2/n with n=35, the number of independent spectral points used for the retrieval) for all spectra. As an example, the reduced χ^2 of the fit of the nadir spectrum with the scaled $HC^{15}N$ profile is equal to 1.018 times that corresponding to the L=3 profile, and for the limb spectrum at 284 km (where profiles differ the most), the reduced χ^2 for the scaled profile is equal to 1.027 times that for the L=3 vertical profile. Thus, the vertical gradient in the $^{15}N/^{14}N$ ratio, retrieved with a relatively small correlation length is not statistically significant. Similar tests were made for the vertical isotopic ratio profile of $^{13}C/^{12}C$ at 15°S, and the two isotopic ratios at 83°N, and we found that isotope vertical profiles proportional to the $H^{12}C^{14}N$ one gave very satisfactory fits of data (with a reduced χ^2 always lower than 1.021 times the one corresponding to the spectral fits with isotopic profiles retrieved with L=3 or 4).

[**Figure 7**]

Additionally, we made several tests to investigate the vertical variations of the isotopic ratios. We tested different vertical gradients for the isotope vertical profiles (keeping the same HCN profile as displayed in Fig. 6). Considering the signal-to-noise ratio, we were not able to constrain any possible increase with height of the $^{15}N/^{14}N$ and $^{13}C/^{12}C$ isotopic ratios, but we could derive a 3-σ upper limit of their decrease with height. The $^{15}N/^{14}N$ vertical variation is not constrained at 15°S, but at 83°N, we found that it cannot decrease by more than a factor of 4 between 170 and 300 km. Concerning the $^{13}C/^{12}C$ isotopic ratio, we conclude that it cannot decrease by more than a factor of 2.5 between 150 and 250 km at 15°S, and a factor of 2 between 170 and 300 km at 83°N.

As no vertical variation of these isotopic ratios is evidenced by the observations, we forced the retrieved vertical profiles of $H^{13}CN$ and $HC^{15}N$ to be proportional to the HCN one in the retrieval process.

3.3.3 The $^{12}C/^{13}C$ isotopic ratio

The inversion kernels corresponding to the retrieved $H^{13}CN$ mixing ratio profile (proportional to the HCN one) are plotted in Figs. 4 and 5, at 15°S and 83°N respectively. At 15°S, like for the HCN inversion, we used both nadir and limb spectra to retrieve the abundance profile of this isotope. The nadir emission of $H^{13}CN$ at 706 cm^{-1} probes levels in the 5-0.20 mbar range (122-265 km) with a maximum at 1 mbar (188 km). The highest part of the $H^{13}CN$ mixing ratio profile is constrained by the emission from 3 limb spectra that probe the 0.3-0.07 mbar range (244-315 km); at higher levels, the signal-to-noise ratio becomes too weak (see Fig. 2 at 350 km).

At 83°N, $H^{13}CN$ was inverted from 8 limb spectra probing levels between 0.95 mbar (165 km) and 0.05 mbar (305 km). Their emissions are optically thin on all limb spectra.

Figure 8 displays the $^{13}C/^{12}C$ isotopic ratios at 15°S (black) and 83°N (gray) relative to

the Earth value (dotted lines) along with the corresponding 1-σ error envelopes (solid line). These error envelopes include uncertainties due to noise, uncertainties on temperature and altitude correction. At 15°S, $^{13}C/^{12}C = (1^{+0.3}_{-0.2})\times[^{13}C/^{12}C]_{\oplus}$ and at 83°N, $^{13}C/^{12}C = (1.3 \pm 0.3)\times[^{13}C/^{12}C]_{\oplus}$.

[Figure 8]

3.3.4 The $^{14}N/^{15}N$ isotopic ratio

Figures 4 and 5 display the kernels corresponding to the the $HC^{15}N$ mixing ratio profile (proportional to the HCN one) at 15°S and 83°N respectively. The $HC^{15}N$ mixing ratio profile is deduced by using the nadir and 4 limb spectra that probe up to 0.04 mbar (357 km). At 711.25 cm^{-1} the nadir emission probes levels comparable to those of the $H^{13}CN$.

At 83°N, $HC^{15}N$ was inverted from 8 limb spectra probing levels between 0.95 mbar (165 km) and 0.05 mbar (305 km).

The deduced $^{15}N/^{14}N$ isotopic ratios at 15°S and 83°N, in Earth value units, are presented in Fig. 8. At both latitudes, the central value of $^{15}N/^{14}N$ (dashed lines) is equal to 4.9 times the Earth ratio, but with differences in error bars and altitude ranges. At 15°S, $^{15}N/^{14}N = (4.9\ ^{+1.5}_{-1.0})\times[^{15}N/^{14}N]_{\oplus}$ and at 83°N it is equal to $4.9\ ^{+0.9}_{-0.7}$ times the Earth isotopic ratio.

4 Discussion

4.1 Temperature profile and HCN vertical mixing ratio profile

As described in Section 3.1, the first guess used in the retrieval process is the HASI temperature profile, which differs from that used in Vinatier et al. (2007). Also, we used a methane abundance of 1.41 % as inferred from the GCMS aboard Huygens, whereas

Vinatier et al. (2007) chose 1.6 % as inferred from CIRS (Flasar et al., 2005). Concerning the temperature profile at 83°N, it can be compared with the thermal profile retrieved at 80°N by Vinatier et al. (2007) from another set of limb spectra recorded earlier in the Cassini mission (during the T3 flyby). The profile retrieved here is generally in very good agreement with their profile in the range where there is information (0.05-1 mbar), except near the 1-mbar level where the temperature in this study is lower by 9 K than what was found from the T3 flyby. The HCN vertical profile we found in this study at 15°S is an update of the vertical profile found by Vinatier et al. (2007), with slight differences due to the temperature profile in the atmospheric model.

At 83°N, the HCN vertical mixing ratio is in agreement with the one derived in our previous work at 80°N (Vinatier et al. 2007), despite the difference in the methane abundance (and thus in the temperature profile) between the two investigations.

We can compare the vertical HCN profile retrieved at 15°S with the profile deduced from ground-based millimeter observations (disk-averaged), which are more heavily weighted towards low latitudes. Our HCN profile is very close to the Hidayat et al. (1997) profile below 200 km, but becomes larger at higher levels (by almost a factor of 2 at 300 km). On the other hand, it is very close to the Marten et al. (2002) profile below 400 km, and larger at higher altitudes.

4.2 The $^{12}C/^{13}C$ isotopic ratio

We have investigated the vertical variations of the $^{13}C/^{12}C$ isotopic ratio at 15°S and 83°N and conclude that it does not decrease by more than a factor of 2.5 in the 150-250 km range at 15°S, and a factor of 2 in the 170-300 km range at 83°N. We therefore constrained the retrieved $H^{13}CN$ vertical profiles to be proportional to the HCN one, which yields good fits of the data within noise level.

At 15°S, we found that the $^{12}C/^{13}C$ ratio is equal 89^{+22}_{-18} (i.e. $[^{13}C/^{12}C]_{15S} = (1\ ^{+0.3}_{-0.2})\times[^{13}C/^{12}C]_{\oplus}$). At 83°N, the retrieved $^{12}C/^{13}C$ isotopic ratio is equal to 68^{+16}_{-12} (which corresponds to $[^{13}C/^{12}C]_{83N} = (1.3 \pm 0.3)\times[^{13}C/^{12}C]_{\oplus}$). The two determinations are thus consistent within error bars. If we combine the two values, we obtain $^{12}C/^{13}C$ = 75 ± 12. Our results obtained near the equator can be compared with the disk-averaged $H^{12}CN/H^{13}CN$ isotopic ratio obtained from ground-based millimeter observations (as most of the information originates from equatorial regions). Hidayat et al. (1997), from their analysis of the (4-3) $HC^{13}N$ rotational line at 345.34 GHz recorded at the JCMT (Mauna Kea, Hawaii), found that for altitudes below 200 km the $^{12}C/^{13}C$ ratio lies between 70 and 120, in agreement with our results (63-87). Gurwell (2004) also determined the $^{12}C/^{13}C$ isotopic ratio in HCN from the same rotational line observed at the Submillimeter Array. He inferred two different results, depending on the temperature profile used in the radiative transfer model. Assuming the Coustenis and Bézard (1995) temperature profile, he retrieved $^{12}C/^{13}C$ = 132 ± 25, while using Lellouch's (1990) thermal profile leads to $^{12}C/^{13}C$ = 108 ± 20. The latter value agrees with our result. However, it should be noticed that the analysis of the ground-based disk-averaged observations assume that the HCN profile does not vary with latitude, which is not true from Voyager and Cassini observations. The analysis of ground based millimeter observations could probably be improved by considering a latitudinal gradient in the HCN distribution.

The $^{12}C/^{13}C$ isotopic ratio was also determined in situ by the GCMS instrument during the Huygens descent in Titan's atmosphere on 14 January 2005. From the methane measurements, Niemann et al. (2005) found a $^{12}C/^{13}C$ isotopic ratio equal to 82.3 ± 1 between 18 and 6 km around 10°S. Waite et al. (2005), from their study of the Cassini/INMS in situ data at 1200 km derived $^{12}CH_4/^{13}CH_4$ = 95.6 ± 0.1, which leads to an estimated value equal to 81 at the surface, in agreement with the GCMS results. The range of the

carbon isotopic ratio found in HCN in this study (between 100 and 350 km) envelops the in situ results relative to CH_4 (the main reservoir of carbon in Titan's atmosphere). As a consequence, it does not appear that carbon undergoes significant fractionation in the HCN formation process.

4.3 The $^{14}N/^{15}N$ isotopic ratio

The vertical variations of the $^{15}N/^{14}N$ isotopic ratio were explored at both latitudes. At 15°S, because of the poor signal-to-noise ratio, they cannot be constrained, whereas at 83°N, we set an upper limit of a factor of 4 on its vertical decrease between 170 and 300 km. We then forced the retrieved $HC^{15}N$ profiles to be proportional to the HCN one, which allows a good reproduction of the data within noise level.

At 15°S, we retrieved a $^{14}N/^{15}N$ isotopic ratio equal to 56^{+16}_{-13} (i.e., $[^{15}N/^{14}N]_{15S} = (4.9\ ^{+1.5}_{-1.0}) \times [^{15}N/^{14}N]_{\oplus}$) , and at 83°N, we retrieved $^{14}N/^{15}N$ equal to $56\ ^{+10}_{-9}$ (i.e.$[^{15}N/^{14}N]_{83N} = (4.9\ ^{+0.9}_{-0.7}) \times [^{15}N/^{14}N]_{\oplus}$). Therefore no latitudinal variations are observed between 15°S and 83°N. If we combine these two results, we obtain $^{14}N/^{15}N = 56 \pm 8$.

This value can be compared with the $^{14}N/^{15}N$ isotopic ratio deduced from ground-based millimeter observations. Marten et al. (2002) studied HCN (at 88.6 GHz) and $HC^{15}N$ (258.16 GHz) among other nitriles and deduced a value for the $HC^{14}N/HC^{15}N$ ratio in the range 60-70. In this study, we obtain an averaged value that lies between 48 and 64, which is in agreement with Marten et al.'s results. Gurwell (2004) also retrieved the $HC^{14}N/HC^{15}N$ isotopic ratio from millimeter observations assuming two different temperature profiles. He derived $^{14}N/^{15}N = 94 \pm 13$ with the Coustenis and Bézard (1995) thermal profile and $^{14}N/^{15}N = 72 \pm 9$ with that from Lellouch (1990). Our results agree with Gurwell's second result within error bars.

The $^{14}N/^{15}N$ isotopic ratio was also determined by the Huygens/GCMS instrument

from N_2 measurements. Niemann et al. (2005) deduced an isotopic ratio equal to 183 ± 5 (between 36 and 41 km), which corresponds to an enrichment of ^{15}N compared to ^{14}N equal to about 1.5 times the terrestrial value. $^{14}N/^{15}N$ was also derived from in situ Cassini/INMS measurements at 1200 km by Waite et al. (2005) who found a value in the range 172-215, corresponding to an estimated value at the surface in the range 168-211, encompassing the GCMS values. The ^{15}N enrichment in HCN is thus higher than in N_2 by a factor of about 3 (considering the GCMS results). As N_2 is the main reservoir of nitrogen in Titan's atmosphere, the higher $^{15}N/^{14}N$ ratio in HCN, a product of the coupled photochemistry of N_2 and CH_4, implies that fractionation processes occur in Titan's atmosphere, which favor $HC^{15}N$ compared to $HC^{14}N$.

As a first step, HCN formation involves, the dissociation of N_2 by extreme UV photons and by electrons. Nitrogen atoms in the ground state (^{4s}N) then react with CH_3 radicals, a direct product of methane photolysis, to form HCN (e.g. Wilson and Atreya, 2004). Reaction of methane with N^+ ions, formed from electron impact and photoionization of N_2, provides another pathway for HCN production. HCN is then diffused to the lower atmosphere and eventually lost by condensation. Incorporation in the photochemical haze has also been proposed as an important loss mechanism for HCN (McKay, 1996; Lara et al., 1999).

Fractionation mechanisms may operate at these different steps. The first one, photodissociation of N_2, may actually be quite efficient. Dissociation of N_2 occurs at wavelengths lower than 100 nm, mostly by a predissociation mechanism, in which a transition occurs to Rydberg and valence states. These states have a long enough lifetime to exhibit vibrational and rotational structure and thus relatively narrow absorption lines (e.g. Haverd et al. 2005, Lewis et al. 2005, Stark et al. 2005). The isotopic shift of the $^{14}N^{15}N$ and $^{15}N^{15}N$ vibration bands relative to the $^{14}N_2$ bands can reach a few tens of cm^{-1} (Sprengers

et al. 2003, Lewis et al. 2005), larger than the linewidth. For continuum irradiation from the Sun, wavelengths corresponding to $^{14}N_2$ line absorption are more rapidly attenuated than those corresponding to the less abundant isotopes. The latter can then undergo photodissociation at levels deeper than $^{14}N_2$ that is self-shielded. This process can potentially increase the $^{15}N/^{14}N$ atom ratio but precise line-by-line calculations, taking into account the solar spectrum, are needed to assess its fractionation effect in Titan.

Fractionation might also occur in the formation reactions themselves (i.e., mostly $^{4s}N + CH_3$ according to Wilson and Atreya 2004) but, to our knowledge, such effects were investigated neither through laboratory measurements nor ab initio calculations. HCN condensation in the lower stratosphere is expected to deplete the heavy isotope in the gas phase as compared with the solid due to isotopic effects similar to those observed for H_2O on Earth. This loss mechanism cannot therefore explain the observed enrichment in (gaseous) $HC^{15}N$. Photolysis is only a minor loss process in Titan's atmosphere as most of the CN radicals are recycled back to HCN. According to Waite et al. (2005), the isotopic fractionation induced by the HCN photodissociation is not sufficient to account for the observed enrichment in $HC^{15}N$. Finally, a possibility is the formation of the photochemical haze if it is a significant loss process for HCN as advocated by McKay (1996), Lara et al. (1999) and Vinatier et al. (2007). Unfortunately, here again, the appropriate laboratory measurements are missing.

5 Conclusions

High-spatial resolution and vertically-resolved data recorded by CIRS allowed us to detect $HC^{15}N$ and $H^{13}CN$ in the infrared range and to retrieve the $^{14}N/^{15}N$ and $^{12}C/^{13}C$ isotopic ratios. The vertical variations of the $^{15}N/^{14}N$ ratio cannot be constrained at 15°S, while at 83°N an upper limit of its decrease between 170 and 300 km was set to a factor of 4. As

concerns $^{13}C/^{12}C$, its decrease with height at 15°S cannot exceed a factor of 2.5 between 150 and 250 km, and a factor of 2 between 170 and 300 km at 83°N. Assuming no vertical variations, the $^{12}C/^{13}C$ ratios inferred at 15°S and 83°N agree within error bars (89^{+22}_{-18} at 15°S and 68^{+16}_{-12} at 83°N). The $^{14}N/^{15}N$ ratio was found equal to 56^{+16}_{-13} at 15°S and 56^{+10}_{-9} at 83°N, i.e. enriched by a factor of 4.9 compared to the Earth. The isotopic ratio values that we obtained here from Cassini/CIRS infrared spectra confirm values derived from previous ground-based millimeter observations. The range in the $^{12}C/^{13}C$ ratio we derived here in HCN encompasses the carbon isotopic ratio in CH_4 deduced in situ from Huygens/GCMS data (82.3 ± 1). We find a enrichment of ^{15}N in HCN that is higher by a factor of about 3 than that in N_2 obtained from in situ measurements, implying the existence of fractionation processes in the HCN photochemistry. Simulations as well as laboratory experiments will be necessary to identify and quantify these processes. Moreover, until the end of Cassini mission, CIRS will extend its coverage over all Titan's surface, which will permit us to improve the accuracy of these isotopic ratios both latitudinally and vertically.

Acknowledgments

We are grateful to the CIRS Investigation Team for their involvment in planning observationnal sequences and data reduction. The study presented here could not have been done without them. We also thank Tobias Owen for his helpful comments. This research was funded by the Centre National d'Etudes Spatiales (CNES), the Centre National de la Recherche Scientifique (CNRS) and the Programme National de Planétologie (PNP) de l'INSU.

Observation	^{12}**C**/^{13}**C**	^{14}**N**/^{15}**N**	**altitude**	**reference**
Ground-based	70 - 120	-	below 200 km	Hidayat et al. (1997)
millimeter	132±25, 108±20	94±13, 72±9	below 300 km	Gurwell (2004)
observations	-	60.5 - 70	below 350 km	Marten et al. (2002)
In situ	82.3±1	-	18.2 - 6.14 km	Niemann et al.
Huygens/GCMS	-	183 ± 5	40.9 - 35.9 km	(2005)
In situ	95.6±0.1	172 - 215	1200 km (in situ)	Waite et al.
Cassini/INMS	81	168 - 211	0 km (estimation)	(2005)
Infrared	89^{+22}_{-18} (15°S)	56^{+16}_{-13} (15°S)	100 - 350 km	this
Cassini/CIRS	68^{+16}_{-12} (83°N)	56^{+10}_{-9} (83°N)	165 - 300 km	study

Table 1: The Earth ^{12}C/^{13}C ratio is equal to 89 and the ^{14}N/^{15}N ratio is equal to 272 (Fegley et al., 1995). Isotopic ratios obtained from ground-based millimeter observations, as well as from CIRS infrared spectra are derived in HCN, whereas GCMS and INMS in situ measurements yield isotopic ratios in CH_4 and N_2.

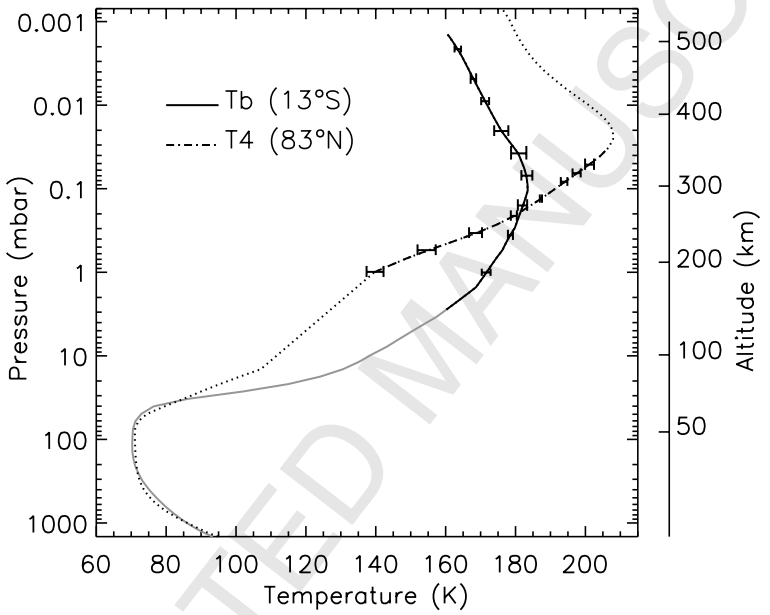

Figure 1: Temperature profiles retrieved at 13°S (Tb, solid black line) and 83°N (T4, dot-dashed line). Parts of the T4 profile in dotted lines are equal to the initial temperature profile given as input of the inversion algorithm; at 13°S the initial guess profile is that deduced from HASI data (Fulchignoni et al. 2005) (solid gray line). The altitude scale refers to the 15°S profile.

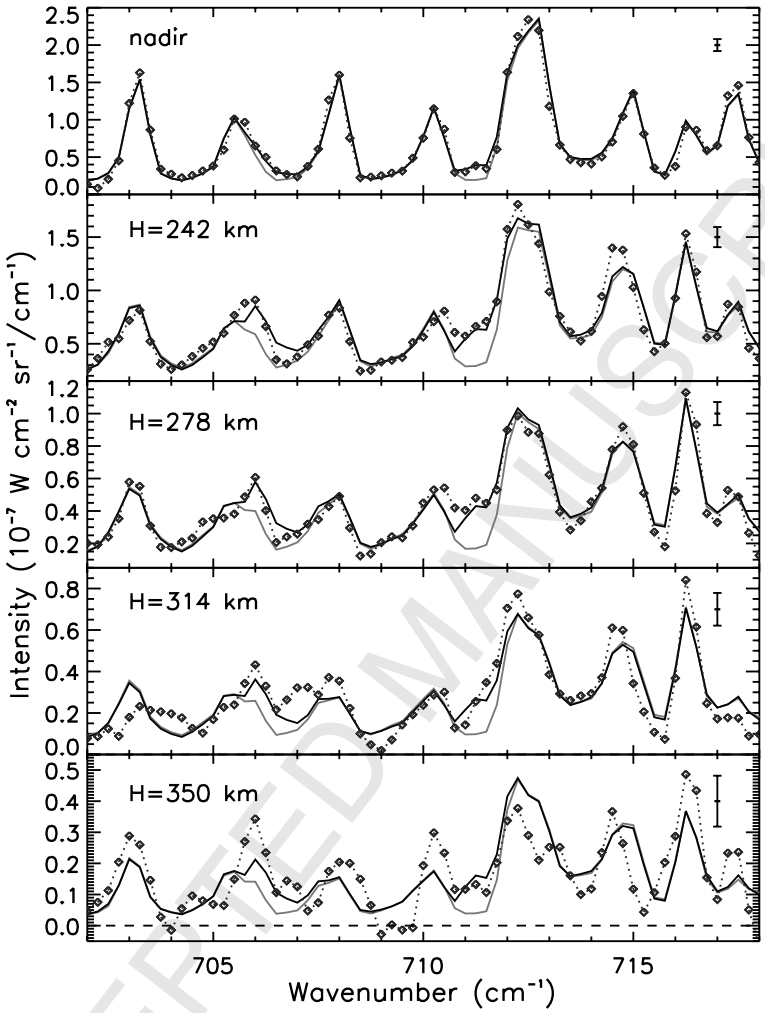

Figure 2: Comparison of the observed spectra (dotted line with diamonds) with calculated spectra that include the HCN isotope emission bands (solid line) and synthetic spectra without the isotope emissions (solid gray line) for nadir and 4 limb spectra at 15°S. Mixing ratio profiles of HCN used here is displayed in Fig. 6, the isotopic vertical mixing ratio profiles are proportional to the HCN one with the ratios $^{12}C/^{13}C = 89$ and $^{14}N/^{15}N = 56$. Detections of $H^{13}CN$ at 706 cm^{-1} and $HC^{15}N$ at 711 cm^{-1} are clear on the nadir and several limb spectra. Error bars equal to the rms of the residuals are indicated for each spectrum (top right).

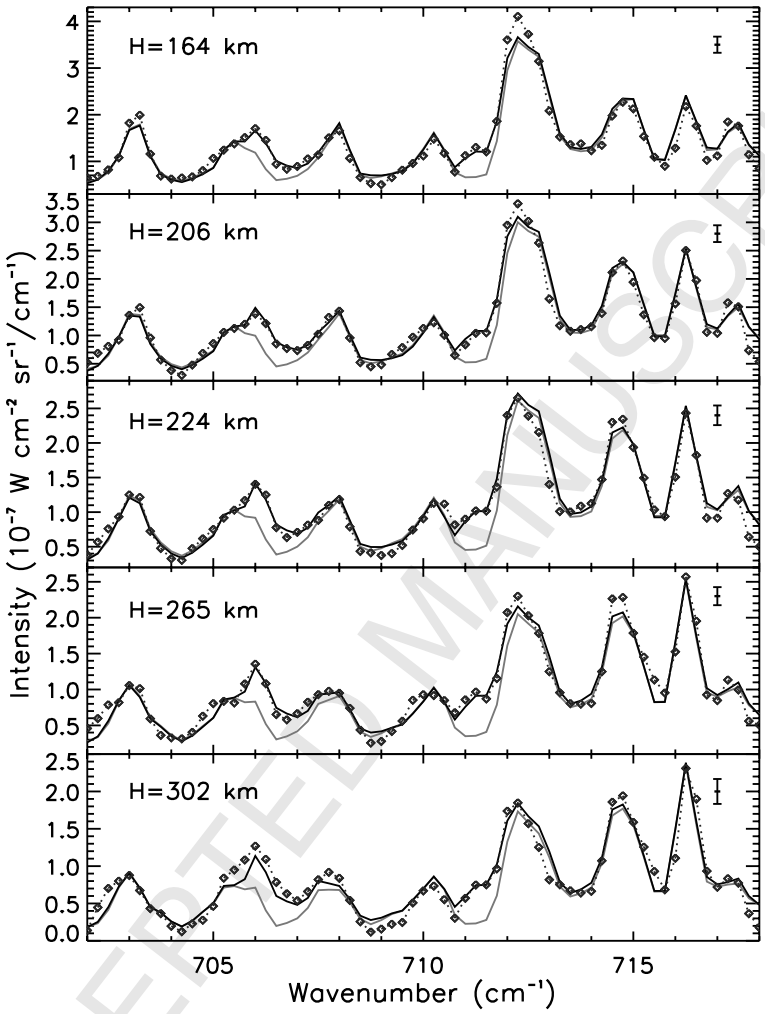

Figure 3: Comparison of the observed spectra (dotted line with diamonds) with calculated spectra that include $H^{13}CN$ and $HC^{15}N$ emission bands (solid line) and synthetic spectra without the isotope emissions (solid gray line), at 83°N, for 5 limb spectra. Mixing ratio profiles of HCN used here is displayed in Fig. 6, the isotopic vertical mixing ratio profiles are proportional to the HCN one with the ratios $^{12}C/^{13}C = 68$ and $^{14}N/^{15}N = 56$. and $HC^{15}N$ are well detectable on several limb spectra. Error bars equal to the rms of the residuals are indicated for each spectrum (top right).

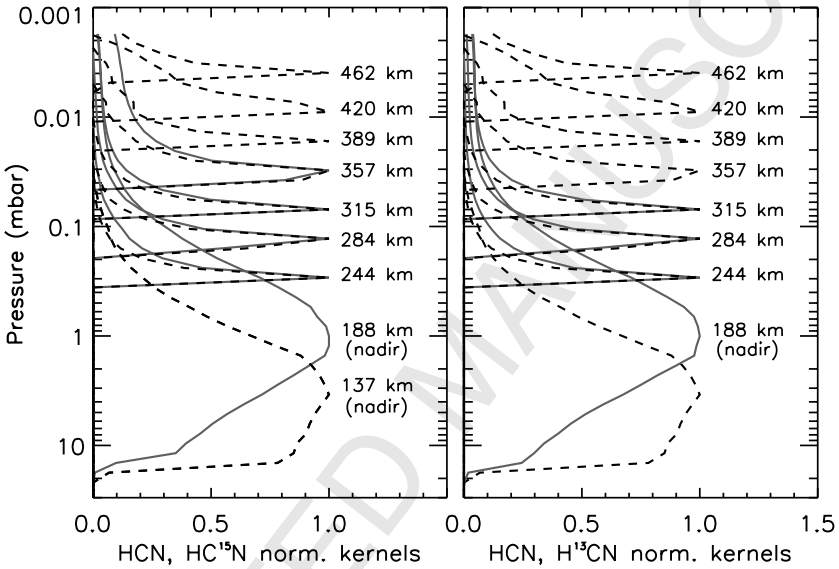

Figure 4: Normalized inversion kernels of $HC^{15}N$ at 711.25 cm^{-1} (left panel, solid gray line) and $H^{13}CN$ at 706 cm^{-1} (right panel, solid gray line) at 15°S, compared in both cases with the $H^{12}C^{14}N$ normalized kernels at 712.25 cm^{-1} (dashed line). Altitudes are given where kernels reach their maxima. The corresponding HCN vertical mixing ratio profile is plotted in Fig. 6. The corresponding $H^{13}CN$ an $HC^{15}N$ retrieved vertical profiles are proportional to the HCN one with $^{12}C/^{13}C = 89$ and $^{14}N/^{15}N = 56$.

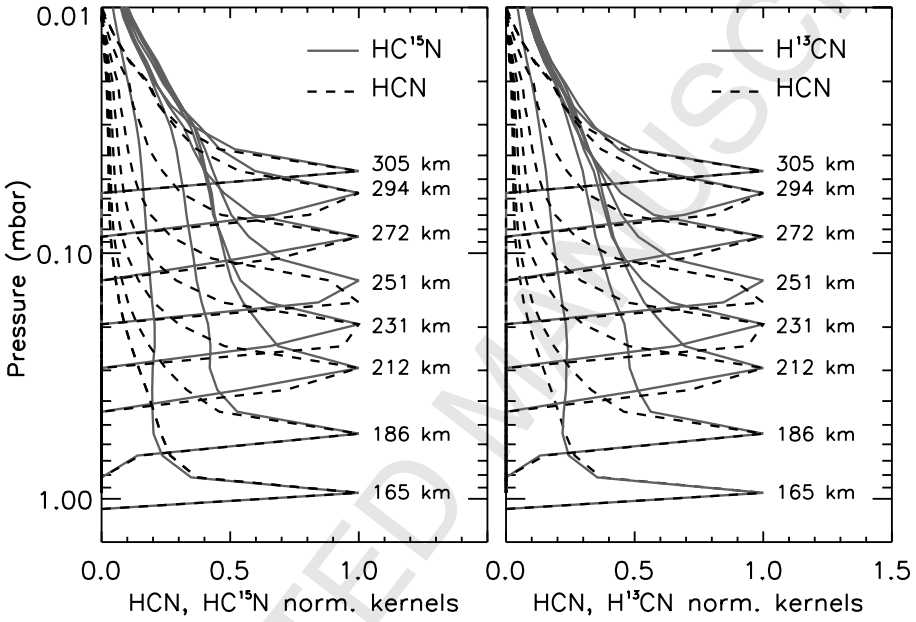

Figure 5: Normalized inversion kernels of $HC^{15}N$ at 711.25 cm^{-1} (left panel), solid gray line) and $H^{13}CN$ at 706 cm^{-1} (right panel), solid gray line) at 83°N, compared in both cases with the HCN normalized kernels at 712.25 cm^{-1} (dashed line). Altitudes are given at kernel maxima of $H^{13}CN$ and $HC^{15}N$. The corresponding HCN vertical mixing ratio profile is plotted in Fig. 6. The corresponding $H^{13}CN$ an $HC^{15}N$ retrieved vertical profiles are proportional to the HCN one with $^{12}C/^{13}C = 68$ and $^{14}N/^{15}N = 56$.

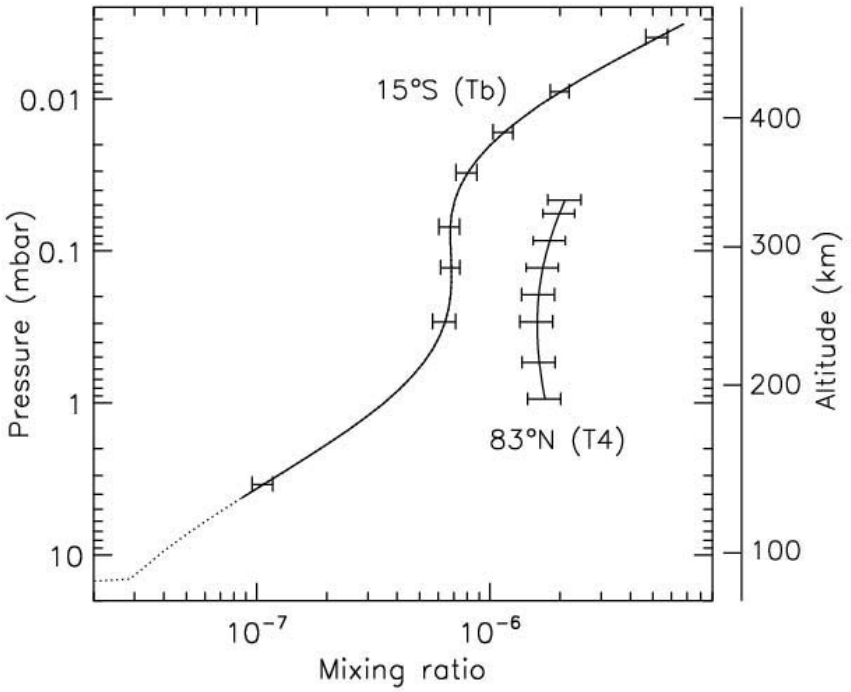

Figure 6: Retrieved mixing ratio profiles of HCN at 15°S and 83°N. Parts where the temperature profile is not constrained are displayed as dotted lines. Error bars (correlated between levels through the filtering of the solution) are plotted at levels where kernels reach their maxima (see Figs. 4 and 5). The altitude scale refers to the Tb profile.

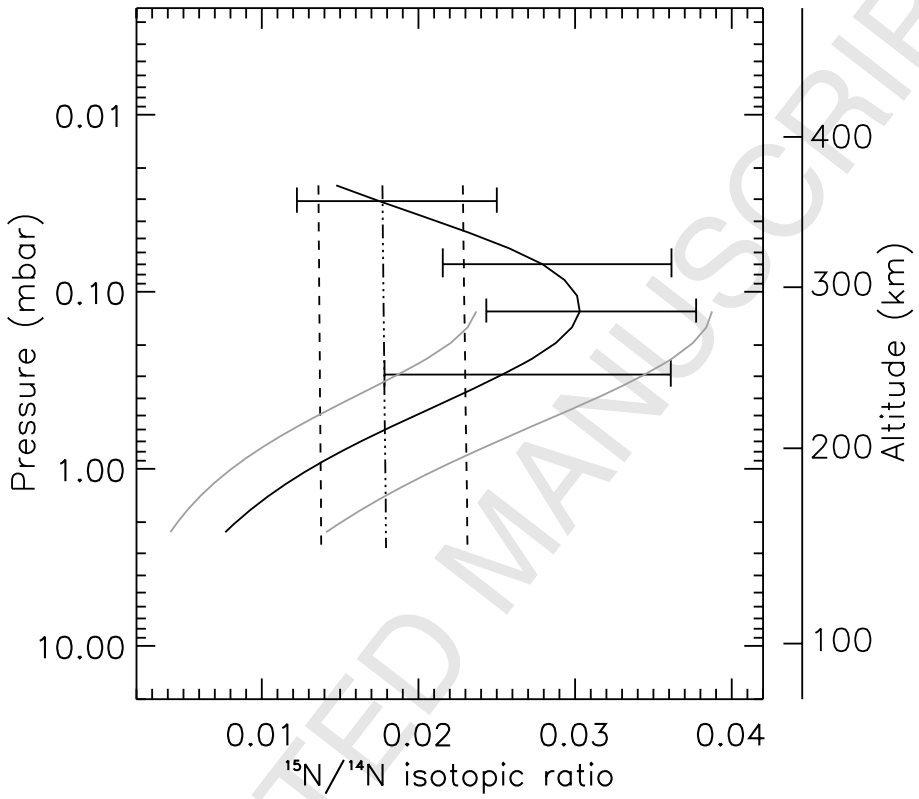

Figure 7: Vertical distribution of the $^{15}N/^{14}N$ isotopic ratio at 15°S. The solid black line corresponds to the isotopic ratio deduced from the vertical abundance profile of HCN displayed in Fig. 6 and a $HC^{15}N$ profile retrieved with a correlation length equal to 3 scale heights. Error bars are plotted at the $HC^{15}N$ kernel maxima. The gray envelope corresponds to the error deduced for the nadir viewing. The dot-dashed line presents the isotopic ratio calculated using the same HCN abundance profile and a $HC^{15}N$ profile proportional to the HCN one. The dashed lines represent the error envelope of this constant-with-height isotopic ratio.

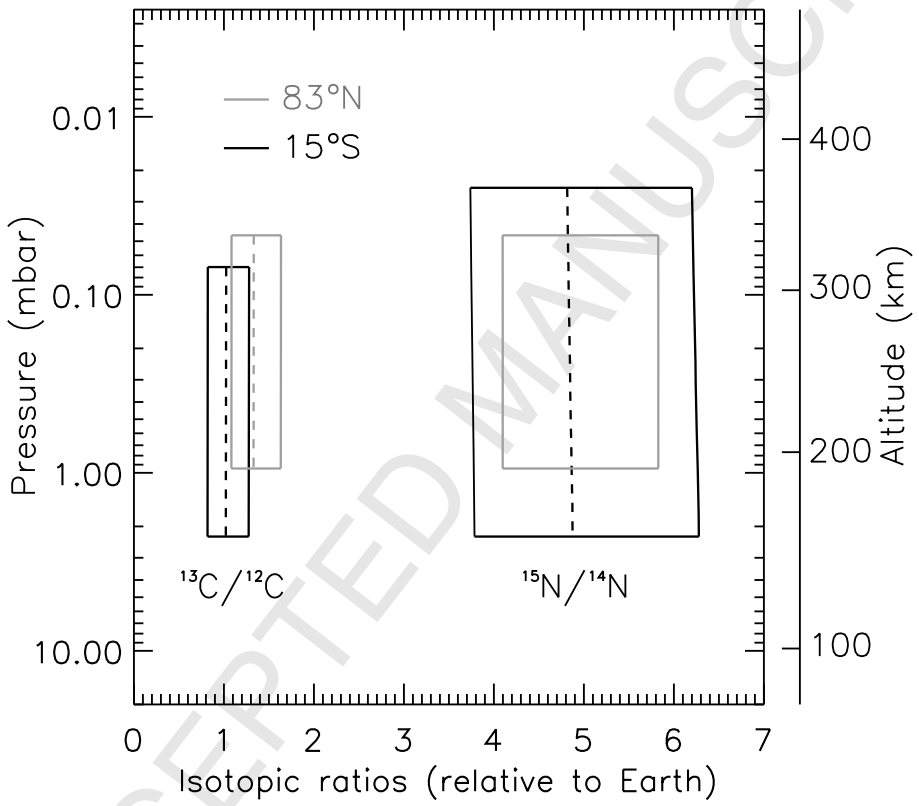

Figure 8: Mean values of the $^{13}C/^{12}C$ and $^{15}N/^{14}N$ isotopic ratios (dashed lines) at 15°S (black) and 83°N (gray) relative to the Earth isotopic ratios. The 1-σ error envelopes are indicated as solid lines. The altitude scale refers to the 15°S profile.